

OCTOPUS: Overcoming Performance and Privatization Bottlenecks in Distributed Learning

Shuo Wang, *Member, IEEE*, Surya Nepal, *Member, IEEE*, Kristen Moore, *Member, IEEE*,
Marthie Grobler, *Member, IEEE*, Carsten Rudolph, *Member, IEEE*, Alsharif Abuadbba, *Member, IEEE*,

Abstract—The diversity and quantity of the data warehousing, gathering data from distributed devices such as mobile phones, can enhance machine learning algorithms' success and robustness. Federated learning enables distributed participants to collaboratively learn a commonly-shared model while holding data locally. However, it is also faced with expensive communication and limitations due to the heterogeneity of distributed data sources and lack of access to global data. In this paper, we investigate a practical distributed learning scenario where multiple downstream tasks (e.g., classifiers) could be learned from dynamically-updated and non-iid distributed data sources, efficiently and providing local privatization. We introduce a new distributed learning scheme to address communication overhead via latent compression, leveraging global data while providing local privatization of local data without additional cost due to encryption or perturbation. This scheme divides the learning into (1) informative feature encoding, extracting and transmitting the latent space compressed representation features of local data at each node to address communication overhead; (2) downstream tasks centralized at the server using the encoded codes gathered from each node to address computing and storage overhead. Besides, a disentanglement strategy is applied to address the privatization of sensitive components of local data. Extensive experiments are conducted on image and speech datasets. The results demonstrate that downstream tasks on the compact latent representations can achieve comparable accuracy to centralized learning with the privatization of local data.

Index Terms—Distributed Learning, Data Collection, Representation Learning, Disentanglement, Privatization



1 INTRODUCTION

The success of machine learning approaches relies on the availability of large datasets [1]. One feasible way to gather massive data is from distributed data sources, enhancing machine learning models. With the prevalence of the Internet of Things (IoT) and 5G networks, a large number of modern distributed devices are incorporated, such as mobile phones, wearable devices, wireless sensors, and autonomous vehicles, resulting in a wealth of data generated in real-time. One of the common data types is high-dimensional data, e.g., high-fidelity images, as a huge number of implementations involve images and videos, such as in video surveillance. Besides, data derived from distributed devices often incorporate sensitive information, such as images or voices, that can be used for re-identification. Transmitting private information from distributed devices raises privacy and data security concerns. Consequently, it is infeasible to directly collect raw data from distributed devices to centralized servers for analysis or model training.

Federated learning has emerged as a training paradigm that enables distributed participants to collaboratively learn a commonly-shared model while retaining data locally, without the need to exchange the data. Federated learn-

ing enables the training procedures to be performed in distributed (federated) learning settings from a group of distributed data sources [2], [3], [4]. However, federated learning approaches are faced with prevailing constraints of Performance and Privatization.

- **Performance of communication:** to retain consensus across the network, distributed nodes have to frequently exchange volumes gradient updates of the sizeable learned model [5], [6], [7] with the server, resulting in expensive communication and scalability constraints [8], [9], especially when devices typically are communication-constrained with limited bandwidth, e.g., IoT devices.
- **Performance of computing and storage:** computation and storage resources of both distributed nodes and servers may not be sufficient to train a complicated downstream model, especially when devices are typically resource-constrained. Besides, multiple downstream tasks need to federated learn multi commonly-shared complicated models from scratch every-time;
- **Performance of accuracy- Heterogeneity of local data bias and data variation with time:** The federated models' accuracy may be degraded by the heterogeneity of local data bias and data variation with time. Due to lack of global data, there is spatial heterogeneity that each node may have a data value bias and data size variation with respect to the general population, and temporal heterogeneity that the distribution of each local dataset may vary with time.
- **Privatization-Additional privacy-preserving strate-**

- Shuo Wang is with the CSIRO's Data61 and Cybersecurity CRC, Australia.
E-mail: shuo.wang@csiro.au
- Surya Nepal, Kristen Moore, Marthie Grobler and Alsharif Abuadbba are with CSIRO's Data61 and Cybersecurity CRC.
E-mail: {Surya.Nepal, Kristen.Moore, Marthie.Grobler and Alsharif.Abuadbba}@data61.csiro.au.
- Carsten Rudolph is with Faculty of Information Technology at Monash University, Melbourne, Australia.
E-mail: Carsten.Rudolph@monash.edu.

gies are required: communicating model updates or collected data contains personally identifiable information (PII) from the local data, requiring additional privacy-preserving strategies. Additionally, the server can be considered as either trusted or not. Further, lack of access to global training data can also cause other security concerns, such as data poisoning or backdoor attacks, or unwanted biases entering the training, e.g., age, gender, sexual orientation.

Autoencoder is adopted as the feature compression approach to address the communication overhead by only transmitting the encoded vector to the server [10], [11], [12]. However, it is often required to train the autoencoder at each distributed node individually, with a limited size of compressed latent codes, resulting in a large number of features being discarded and a heavy computing burden for every node. Consequently, it is important to investigate a practical distributed learning scenario where multiple downstream tasks (e.g., classifiers) could be learned from dynamically updated and non-iid distributed data sources, efficiently and providing local privatization. However, existing federated learning schemes failed in this scenario due to the bottlenecks mentioned above.

To reduce the communication burden and take advantage of global data while addressing privatization, we propose a novel distributed learning scheme inspired by the octopus. An octopus has a brain that serves as a nerve center but contains only 40 percent of its brain cells. The remaining 60 percent are present in its eight arms, as eight ‘mini-brains.’ The octopus uses receptors and suckers on each arm to obtain environmental information. The arms can carry out simple learning and act independently, sending abstract information to the brain to learn higher-level decision-making processes. This solution gives the octopus extremely efficient cognitive abilities beyond the average animal. Similarly, our OCTOPUS learning scheme distributes the feature extraction and encoding at edge nodes while gathering encoded codes and learning downstream models at the server. Compared to ordinary federated learning and centralized learning, the OCTOPUS framework addresses bottlenecks towards a practical distributed learning with multiple downstream tasks and dynamically-updated and non-iid distributed data sources and has the following advantages:

(1) The OCTOPUS addresses communication performance overhead without significant deterioration in the quality of representation. It uses Distributed Vector Quantized Autoencoder (DVQ-AE) to enable distributed encoding at edge nodes to extract expressive compressed representation features transmitted as a set of low-dimensional discrete indices.

(2) The OCTOPUS experiences minimal accuracy performance degradation, addressing the lack of global data. It applies Group and Sliced Vector Quantization and Flexible and Stabilized Training to handle the heterogeneity of local data bias and data variation with time and update the individual DVQ-AE for each distributed participant continuously.

(3) The OCTOPUS balances the computation and storage performance via training distributed DVQ-AE between the nodes and server and places the training of downstream

models, e.g., classifier, using latent codes at the cloud only, avoiding subjection to the complexity of models and constraints of the node devices.

(4) To address the privatization of local data, the disentanglement strategy is incorporated in OCTOPUS to automatically distinguish components that may be subject to PII, without introducing additional cost due to encryption [13] or perturbation [14] required in federated learning. Based on the disentanglement, a general DVQ-AE model can be trained at the server using public-available data (e.g., celebrity profile images). Each distributed participant can only release the user-specific non-sensitive latent codes to the server. Without sensitive latent codes, the server can only reconstruct non-sensitive information using the gathered latent codes.

We conduct extensive experiments on Image (MNIST and CelebA) and Speech. The results demonstrate the comparable accuracy and privatization of our approach with a smaller transmission and local privatization burden compared to ordinary federated learning and centralized learning.

2 OCTOPUS LEARNING FRAMEWORK

2.1 Problem Formulation

The scope of the work is towards a practical distributed learning scenario where multiple downstream tasks could be learned from dynamically-updated and non-iid distributed data sources. Intuitively, we hope to learn a global feature dictionary, and distributed local encoder to map a high-dimensional sample to the indexes of the dictionary, then transmit the index matrix and learn multiple downstream tasks on the gathered compressed features. To address local data bias and dynamic updates, the dictionary is expected to be updated easily. Further, plug-in privatization of local data could be achieved by forcing the global dictionary only to be the carrier for the commonly-shared features.

There are many practical scenarios, for example, speech-to-text recognition, which is our organization’s current industrial implementation of OCTOPUS. Speech consists of content (phonemes) and style (speaker identification). We have demonstrated that the global dictionary learned for speech can be highly related to phonemes with little speaker identification information. The same sentence spoken by different speakers would thus be projected to a similar dictionary item. Therefore, the local encoder could map the speech to the index of the dictionary instead of the raw speech. And the dynamic dictionary update could handle the spatial and temporal bias of local data. Multiple downstream tasks could be conducted on the gathered compressed features via a simple model and less computation than raw data.

Formally, we consider the problem setting where a stream of gathering samples $x \sim D_i$, $x \in \mathbb{R}^n$ is continuously and independently collected from M different distributed devices D_i , $i = 1, \dots, M$, to a server for model training. The diversity and quantity of the training data, collected from distributed devices at a high frequency, largely determines the final model’s robust performance. It is expected to collect the distributed information without

the communication overheads and concerns about the personally identifiable information x^s could be inferred from the transmitted \hat{x} . Besides, the compressed representations that reveal most of the important features of the local data could address the computation and storage concerns.

To address the performance and privatization concerns mentioned in the introduction, we propose the OCTOPUS distributed learning scheme that is designed to have the following properties:

(a) **Encoding:** transforms raw data to low dimensional latent space compressed representation features (latent codes for short) for transmission and computing, $E : X \rightarrow Z$ and $Z \in \mathbb{R}^k$, $k \ll n$, to address the communication constraints. This encoding is characterized by the conditional probability distribution $P_{Z|X}$;

(b) **Disentanglement:** the encoder is incorporated with an additional disentanglement strategy to facilitate the decomposition of the latent representation, Z , into a public component Z_\bullet irrelevant to PII, and a private component Z_\circ relevant to PII, i.e. $DT(Z) = Z_\circ + Z_\bullet$, to address privatization on local data. Specifically, we isolate information about sensitive and non-sensitive attributes into separate subspaces, while ensuring that the latent space factorizes these subspaces independently.

(c) **Flexible and Stabilized Training:** all collected latent codes Z are stored and used for training of downstream models T_i , e.g. classifier at the cloud. The compressed version of global data could address the computing and storage overheads while taking advantage of the global data. The encoding mechanism training is expected to take a small communication and computation resource allocation for each distributed node while enabling the continuous update.

2.2 Overview of OCTOPUS

As shown in the Figure 1, the workflow of the OCTOPUS is:

- Step 1. Learn an initial global Autoencoder (DVQ-AE) on a relevant public-available dataset at the server: learn a global feature dictionary (consisting of K items with dimension D), encode an input to $M \times M$ feature vector with dimension D , and find the index of the most similar dictionary item for each feature vector, resulting in $M \times M$ index matrix as the compressed features.
- Step 2. One-shot locally fine-tuning with distributed encoders and a joint decoder for the local DVQ-AE at each participant in a distributed manner using the initial global DVQ-AE and local data, fixing the global dictionary.
- Step 3. The disentanglement strategy is used to peel PII from the encoded latent codes. Based on the disentanglement, each distributed participant can release only the latent codes' non-sensitive components to the server, without concerns of releasing sensitive information or the additional cost of encryption or perturbation.
- Step 4. Local encoder transmits low-dimensional compressed features of collected samples at a higher frequency.

- Step 5. When new data comes in, the distributed autoencoder will be continuously updated by updating the local codebook via a simple exponential moving average, instead of retraining the local encoder and decoder, and then sent to the global dictionary at a lower frequency.
- Step 6. Multiple downstream task learning could be conducted on the gathered compressed features via simple models at the server. If required, the simple inference model could be returned to the node for real-time inference.

OCTOPUS consists of the basic Distributed Vector Quantized Autoencoder (for general communication, detailed in Section 2.3) and three performance enhancement strategies: Group and Sliced Vector Quantization (for accuracy performance, detailed in Section 2.4), Disentanglement (for privatization performance, detailed in Section 2.5), and Flexible and Stabilized Training (for computing and storage performance and continuously updating, detailed in Section 2.6) strategies. The basic Distributed Vector Quantized Autoencoder consists of an encoder E , a vector quantization operation VQ , and a decoder D . E maps the sample into latent representation. VQ finds the nearest embedding from a learned codebook for each latent representation vector to generate a discrete latent code using the embedding index. D decodes latent embedding back to input space. Each participant's high-dimensional collected data will be processed locally to reduce the dimension with the fine-tuned encoder to take advantage of the data locality at each node. The most critical features in the data are extracted via the local encoder, and the dimension of the input data is reduced by low dimensional latent codes. We learn and transmit the expressive encoded latent codes of the data in the client stage with local privatization through the additional disentanglement strategy. The actual downstream task, e.g., classification, is performed in the server stage using the collected latent codes, alleviating computing, and storage overheads. If required, the privacy-preserving representation of the raw data can be reconstructed at the server using the latent codes and the fine-tuned decoder.

2.3 Basic Vector Quantized Procedure

The basic encoding function is introduced in this section. For the DVQ-AE, the encoder maps the sample x into latent representation $E(x) = Z_e(x) \in \mathbb{R}^{h \times w \times M}$, where $h \times w$ is the size of the embedded feature map of one kernel, and M is the number of kernels. The vector quantization operation finds the nearest embedding $e_i \in \mathbb{R}^M$ from the learned codebook $e \in \mathbb{R}^{K \times M}$ (K vectors of size M) for each M -dimensional vector of $z_e(x) \in Z_e(x)$, using the index $[i]$ of e_i to construct the discretized latent codes $z(x) \in [K]^{h \times w}$. The decoder D maps $z(x)$ to corresponding embeddings $z_d(x) \in \mathbb{R}^{h \times w \times M}$ of the codebook, and decodes $z_d(x)$ back to input pixel space. The learning objective of DVQ-AE is given as:

$$L = \|x - D(z_q(x))\|^2 + \alpha \|sg[z_e(x)] - e\|^2 + \beta \|z_e(x) - sg[e]\|^2 \quad (1)$$

The first term is a reconstruction loss, defined as $-\log p(x|z_q(x))$ which is the negative log likelihood of decoder output x given the output of the encoder $z(x)$

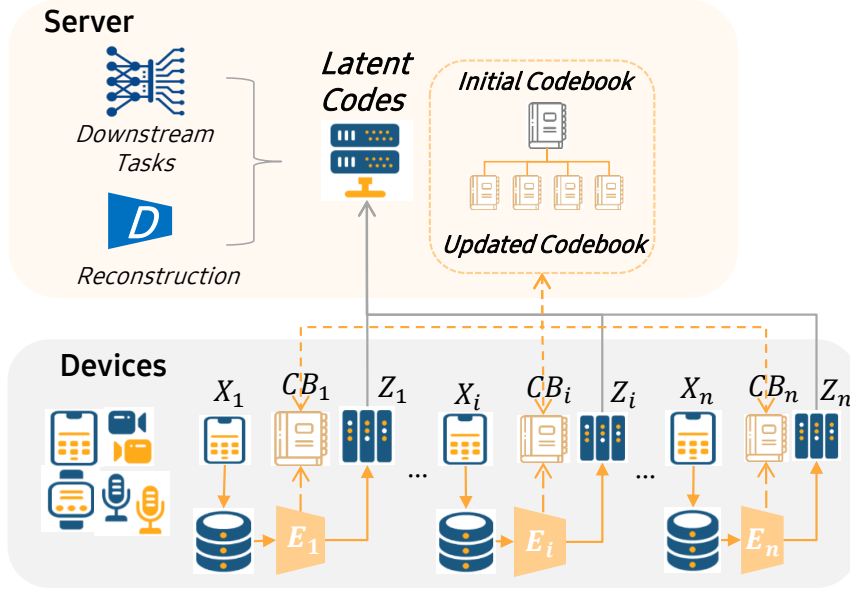


Fig. 1. The OCTOPUS learning framework.

after quantization q . The second term is codebook loss that guides VQ embedding vectors e (called atom hereinafter) towards encoder output $z_e(x)$. The purpose of the VQ term is used to guarantee that embeddings are also guided by reconstruction loss. The third term is the commitment term to make the encoding commits to a VQ embedding vector e and constrain how the VQ space is used. Here $sg[]$ is the stop gradient operator, maintaining its argument during the forward pass and returning zero gradients during backward pass. The gradient of this non-differentiable step is approximated using the straight-through estimator.

2.4 Group and Sliced Vector Quantization (GSVQ)

As the first enhancement of DVQ-AE, this strategy is used to increase the accuracy performance affected by the spatial and temporal heterogeneity of local data. No constraint on the atoms' distribution is placed in the embedding dictionary for general VQ-VAE so that adjacent atoms can represent totally different features. To mitigate the distortions caused by the mismatch of atoms, a Group Vector Quantization (GVQ) is adopted by GSVQ to decrease the probabilities of quantizing the encoder's output to a mismatched atom, similar to group sparse coding algorithms [15]. GVQ aims that similar atoms are closer to each other, and different atoms are further away.

GVQ divides the codebook $e \in \mathbb{R}^{K \times M}$ into G groups along K dimension, and $e^{(i)} \in \mathbb{R}^{N_g \times M}$, $N_g = \frac{K}{G}$ denotes the i -th group. During forward-propagation, each output of the encoder $z_e(x)$ is mapped to the nearest atom group, based on the average distance over all the atoms in the group.

$$e^* = e^{(j)}, \text{ where } j = \underset{k}{\operatorname{argmin}} d(z_e(x), e^{(k)})$$

$$d(z_e(x), e^{(j)}) = \frac{1}{M} \sum_{k=1}^M \left\| z_e(x) - e_k^{(j)} \right\|_2 \quad (2)$$

The corresponding i^{th} index of latent code for $z(x)$ is then computed as the weighted average of the atoms in the e^* .

$$z(x)_i = \frac{\sum_{k=1}^M w_k e_k^*}{\sum_{k=1}^M w_k}, \quad w_k = \frac{1}{\|z_e(x) - e_k^*\|_2} \quad (3)$$

All atoms will be updated in the back-propagation, based on the loss in Equation (1), by replacing e^* with $\frac{\sum_{k=1}^M w_k e_k^*}{\sum_{k=1}^M w_k}$.

In addition, Sliced Vector Quantization (SVQ) [16], [17] is adopted by GSVQ to further improve the efficiency of nearest neighbor embedding. Each atom of the codebook is separated into n_c parts along the M dimension, i.e. $e = \{e^j \in \mathbb{R}^{K \times M/n_c}\}_1^{n_c}$. Accordingly, the output of encoder $z_e(x)$ is divided along the M dimension into n_c components and the VQ procedure is conducted in terms of the separated codebook at the corresponding spatial location. Figure 2 presents the GSVQ diagram.

2.5 Disentanglement for Local Privatization

To address the privatization of the local data, we first apply an unsupervised disentangled strategy to force the codebook as the carrier for the commonly-shared features only (public component), while learning to represent private components such as speaker identification by the information discard the quantization, i.e., the difference between continuous space and the discrete codes.

A well-trained vector quantized model can learn some commonly-shared features as a similar series of atoms of the codebook. For example, the codebook learned for speech can be highly related to content such as phonemes [18], [19], [20]. The same sentence spoken by different speakers would thus be projected to a similar codebook series. We assume that the latent codes of instances consist of a public component (e.g., speech-to-text recognition) and a private component (speaker identification). It is preferred to obtain better disentangled latent codes by stripping the private components.

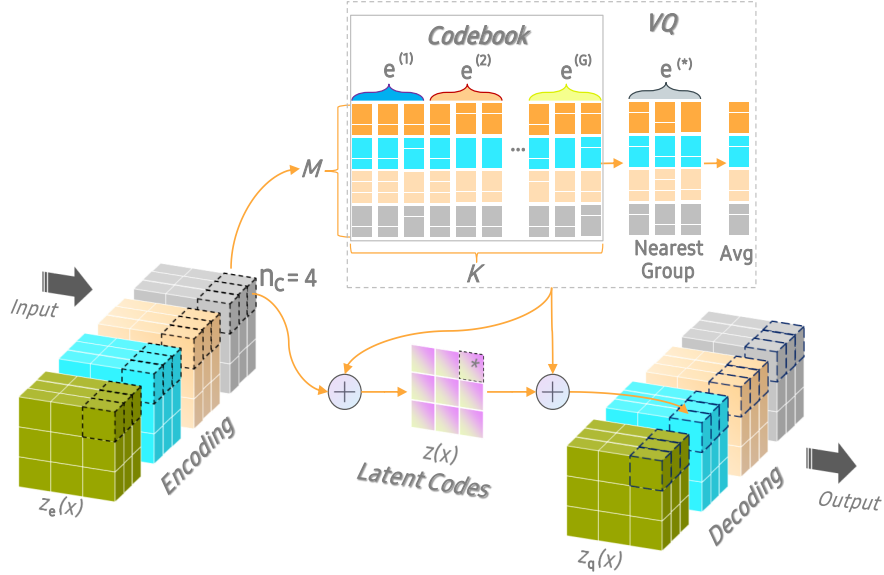


Fig. 2. The GSVQ framework.

The public component Z_\bullet and private component Z_o is given as

$$Z_\bullet = VQ(E(x)), Z_o = E[E(x) - Z_\bullet] \quad (4)$$

Here, Z_o can be considered as the expectation of difference between $E(x)$ and its vector quantized codes Z_\bullet .

Accordingly, the reconstruction loss in Equation (1) is updated to be

$$L_{rec} = E_{x \sim X} [\|D(Z_\bullet + Z_o) - x\|] \quad (5)$$

An Instance Normalization (IN) layer is added before the VQ step to filter more information about the private component. Figure 3 shows the framework of disentanglement strategy.

The disentanglement strategy can be incorporated into the initial DVQ-AE training at the server. The data owner can then have privatization on the local data by either incorporating the sensitive component or not.

To further disentangle the latent representation, we apply Hierarchical Latent Codes, utilizing a hierarchy of vector quantized codes [21] to model data. A top latent code is used to model global information, and a bottom latent code, conditioned on the top latent, is used to model local details. The disentanglement strategy is only applied to the top latent code.

2.6 Flexible and Stabilized Training

This strategy is used to improve computing and storage performance and continuously update local and global encoder/decoder/codebooks. The distributed DVQ-AE at each node is fine-tuned by alternately updating the distributed encoder, joint decoder, and codebook on local data. Initially, the codebook is frozen and updated at a lower frequency. The local encoder and joint decoder have a fixed update frequency, using local data to fine-tune. Fine-tuning the codebook can also address the drifting representation issue when the current DVQ-AE is not a good approximation for new data. The local codebook can be fine-tuned by

updating the atoms of the codebook with an exponential moving average instead of the loss term [20], where it was used to reduce the variance of codebook updates. Specifically, $\{z_{i,1}, z_{i,2}, \dots, z_{i,n_i}\}$ denotes the set of n_i outputs from the encoder that are closest to atom e_i in the codebook so that the loss used to update the local codebook is:

$$\sum_j^{n_i} \|z_{i,j} - e_i\|_2^2 \quad (6)$$

The optimal value for e_i is simply the average of elements in the set:

$$e_i = \frac{1}{n_i} \sum_j^{n_i} z_{i,j} \quad (7)$$

The exponential moving average procedure is conducted as:

$$\begin{aligned} N_i^{(t)} &:= \gamma N_i^{(t-1)} + (1 - \gamma) n_i^{(t)} \\ m_i^{(t)} &:= \gamma m_i^{(t-1)} + (1 - \gamma) \sum_j z_{i,j}^{(t)}, e_i^{(t)} := \frac{m_i^{(t)}}{N_i^{(t)}} \end{aligned} \quad (8)$$

with $\gamma = 0.99$. The codebook update is conducted in a relatively lower frequency, such as monthly updates using the weekly samples $e_i^{(t)}$, then sent to the server.

3 EXPERIMENTS

3.1 Datasets and Settings

We present the results of experiments on the MNIST [22], CelebA [23] (resize to 128×128) and Speech [24] datasets to demonstrate the effectiveness of our approach in terms of performance on performance and privatization. We assume the server's downstream tasks are attribute classification for MNIST (containing a circle or not) and CelebA (gender and smiling), and phoneme identity accuracy for SPEECH, respectively. The latent codes collected from distributed nodes are input to train the classifier for classification or text recognition at the server. We split all samples into the training set Tr (80%) and hold out the rest as a test set Te (20%). 85% of the Tr is used as the centralizing training data

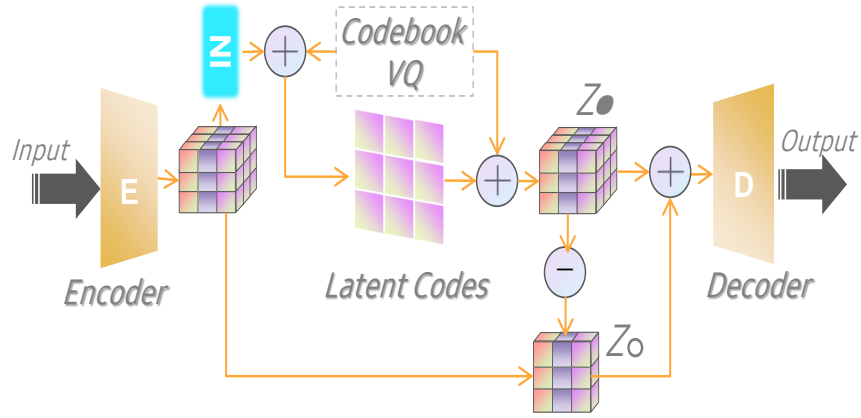


Fig. 3. The disentanglement strategy framework

(CTD), and the remaining 15% is used as the additional data (ATD, e.g., as the public-released relevant datasets).

A three-scenario evaluation is adopted to validate the performance of OCTOPUS.

Centralized scenario: The set of uncompressed CTD data is used as the entire collected data to train the downstream tasks in a centralized manner. Then, the test set is used to evaluate the performance metrics to set the baseline.

Federated scenario: The CTD dataset is divided into different subsets as the distributed data sources for federated learning to train the same downstream tasks. The test set is then used to obtain the needed performance metrics. For an independent and identically distributed (IID) setting, each node is randomly allocated a uniform distribution over all classes. For a non-IID setting, the data is sorted by class, and each node receives data partition from only a single class. The same notations for FedAvg algorithm in [25], [26] are adopted. We apply 100 clients, each running one local epoch on top of 100 global communication rounds. We also evaluate the performance when the federated learning is incorporated with differential privacy to address the privacy of personally identifiable information, at $(\epsilon, \delta) = (10, 10^{-5})$ -DP.

OCTOPUS scenario: The ATD dataset is used to train the initial DVQ-AE, followed by fine-tuning using the distributed data source (used in the federated scenario). Each sample from every distributed data source is mapped to the node-specific autoencoder’s encoder. The server gathers the encoded latent codes to be the training set to train the same downstream tasks. After that, the model’s performance evaluations are obtained using the encoded version of the test set.

In our experiments we explore four group setups for the codebook structure with $N_v = 1, 4$ and $N_h = 1, 41$, respectively. Let the codebook size B_x reveal the compression ratio, and each group setup is conducted on B_{32} , B_{64} , B_{128} , B_{256} , and B_{512} settings.

3.1.1 Performance Metric

The following quantitative metrics assess the effectiveness of the OCTOPUS framework. (1) The first metric is the test accuracy of the downstream task models obtained after the training process. Classification accuracy is used for images and 1 - Word Error Rate (WER) for speech. (2) We

trained an identifiable information classifier, consisting of three Conv1d layers with 256 hidden nodes and a fully connected layer on the last layer, to classify the PII on discrete content embedding. The predictability of PII from released latent codes, i.e., the classification accuracy of the identifiable attribute, is used to evaluate privatization. (3) Taking the same identifiable information classifier, we test the recognition accuracy of identification using a set of samples with identifications excluded in the training and testing dataset on various sizes of embedding codes, as the degree of disentanglement metric. (4) The training and testing time and the compression ratios are also investigated as evaluation metrics.

The frame of the encoder of DVQ-AE consists of two stridden conv layers with ReLU, stride 2 and 4×4 kernel, succeeded by a conv layer with 3×3 kernel, the same padding, followed by two residual blocks (ReLU, 3×3 conv, ReLU, 1×1 conv). The decoder has a symmetrical structure, composed of 2 residual blocks, succeeded by 2 transposed convolutions with stride 2 and 4×4 window size. The design, training, and testing of the deep learning models (Autoencoders and CNN Classifiers) were implemented using the Keras deep learning framework on a TensorFlow backend, running on NVIDIA Tesla P100 GPU.

We take the premise for the initial global estimation only (cold start problem). Besides, we prefer to provide and take advantage of the pre-trained model as the start, then only fine-tuning is required for our scheme. For example, the speech pre-trained initial model could be used for most speech recognition scenarios. We have validation subset for the initial global model training. Most of the hyper-parameters are learned at initial learning and directly used for the following procedures, such as distributed fine-tuning.

3.2 Effect on Test Accuracy on Downstream Tasks

We evaluate downstream task models’ testing accuracy when trained and tested in Centralized, Federated, and OCTOPUS scenarios with MNIST, CelebA, and Speech datasets.

Figure 4 illustrates the comparison of the downstream task models’ testing accuracy in the OCTOPUS scenario using various compression ratios, compared to centralized and federated scenarios. The testing accuracy for the centralized scenario (uncompressed data), the baseline of accuracy, is

highest across all the cases, as all features in the raw data can be utilized to train models. Furthermore, the testing accuracy for OCTOPUS is higher than that of Federated in the non-IID and privacy-preserving settings on all three datasets. It is also found that the more complex the image, the more significant the gap. As shown, there is a general degradation in the testing accuracy when the compression ratio increases from B_{512} to B_{32} , as the number of features utilized to train models is decreased. Namely, a smaller compression ratio means the model has more features to train a stranger model.

The rate of reduction of the model’s testing accuracy varies across the models on two image datasets, with MNIST as the highest for all the compression ratios. The reason is that the number of features for the simple data of small dimensions is even smaller than encoded features. The significant degree of degradation is also observed in Speech, as the complex downstream task needs more features to train the model. We further demonstrate that there is significant degradation of the utility for federated learning in the non-IID scenarios (approximately 10%-30% drop in the downstream task accuracy) and after incorporating the privacy-preserving procedure (approximately 30%-50% drop in the downstream task accuracy). The OCTOPUS avoids such degradation by incorporating advantages from both centralized learning and federated learning.

For the MNIST dataset, as shown in Figure 4, original samples can easily be recognized with more than 99% accuracy on average for the centralized scenario. However, the privacy-preserving centralized case has obviously lower accuracy than expected compared to the centralized scenario. Even under B_{32} compression ratio, the accuracy of OCTOPUS is generally better than that of the centralized learning with DP and federated in non-IID and with DP cases. For the CelebA dataset, the classifier trained on the centralized case can achieve around 90% test accuracy on both utility tasks (gender and smiling) on average, while our trained downstream task using OCTOPUS can achieve a comparable accuracy (87% on average) on the compact latent representations. The accuracy of OCTOPUS is better than that of the centralized learning with DP (82% on average) and federated in non-IID (51% on average) and with DP (30% on average) cases. The evaluation on Speech confirms that OCTOPUS does not degenerate the utility of the expected downstream task too much compared to the centralized scenario and is better than the federated scenario.

3.3 Effect on Privacy

For the MNIST datasets, the digit number itself is considered as the private component. The digit either contains a circle (i.e., digits 0,6,8,9) or not as the downstream recognition task. Figure 5 demonstrates samples of the (a) original dataset along with the corresponding (b) reconstructed version via the DVQ-AE to remove information on the digit identity while keeping the circle recognition information. We further evaluate the accuracy of distinguishing PII. The classification accuracy on the private component decreases quickly, from 95% to below 10%, while classification accuracy on the circle recognition remains nearly similar to

the centralized scenario. This means the OCTOPUS does not degenerate the utility of the expected downstream task too much while significantly restraining the privacy leakage about the PII.

For the CelebA dataset, we consider the identification as the privacy component, and the gender and smiling recognition as the two downstream tasks used the model in [27], [28]. As shown in Figure 6, the OCTOPUS model can reduce the test accuracy of private information (identification) from 85% down to around 10% on average, demonstrating the ability to protect private information. It demonstrates that the privatized data can still serve the desired classification tasks at the cost of only a small utility accuracy (4% drop). We also demonstrate the samples of the reconstructed identification-privatized face images in Figure 5, which shows the desired phenomenon that the identification is blurry while remaining the utility attributes (gender or smiling).

For the Speech dataset, we consider the speaker’s identification as the privacy component, the phoneme identity as the downstream task used the model in [24]. The evaluation of Speech confirms that OCTOPUS significantly reduces the privacy leakage about the PII.

We also compare the privatization performance of OCTOPUS with centralized learning and private federated learning incorporated with differential privacy. As shown in Figure 6, the inference probability of personally identifiable information for OCTOPUS (between 10-20%) is much better than the other (between 30-80%), without introducing additional cost due to perturbation.

3.4 Effect on Disentanglement

Taking the Speech recognition scenario as an example, we test the privacy component’s recognition accuracy using speaker voice excluded in the training dataset, as the degree of disentanglement of OCTOPUS. The results are summarized in Figure 7. The test accuracy of speaker identification is reduced by half on the codebook size for OCTOPUS, compared to the same scheme without our disentanglement strategies. This demonstrates that the latent codes would cause privacy leakage, e.g., speaker information. Namely, the fewer codes in the codebook, the less the privacy component is incorporated. The recognition accuracy increases as the codebook size is enlarged from 32 to 512. However, the re-identification accuracy remains at low probability, even with the B_{512} codebook size. We find there is a trade-off between the disentanglement and utility of codes for downstream tasks. If we compress the codebook into only a few codes, the disentanglement ability is strong while being hard to contain sufficient features of content information. In our experience, B_{256} is a proper size of codebook to balance the trade-off. These experiments demonstrate that the OCTOPUS scheme can achieve good disentanglement performance without explicitly incorporating any objective or constraint to the encoder or decoder.

3.5 Effect on Other Performance Improvements

The improvements in communication, computing, and storage performance are intuitive. For example, DVQ-AE can compress the high-dimensional raw face image with $128 \times$

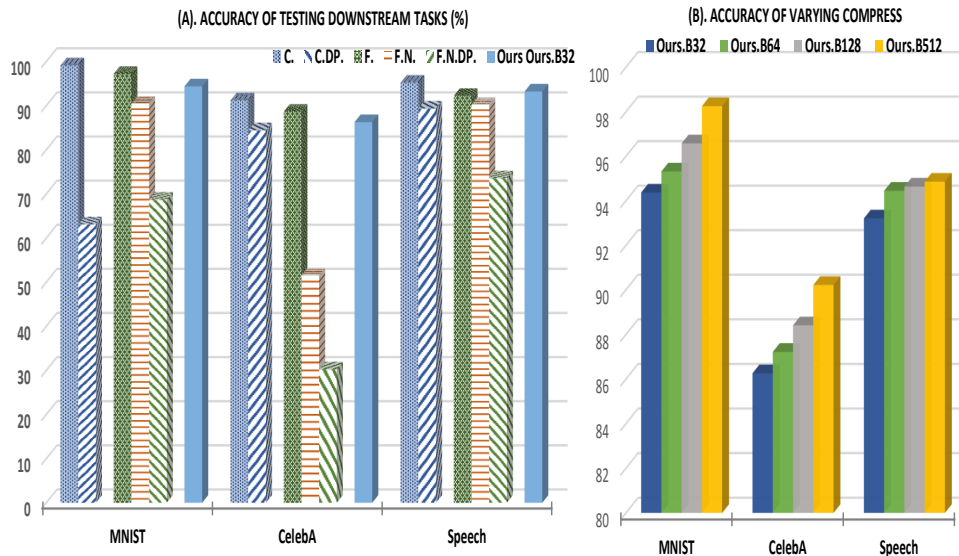
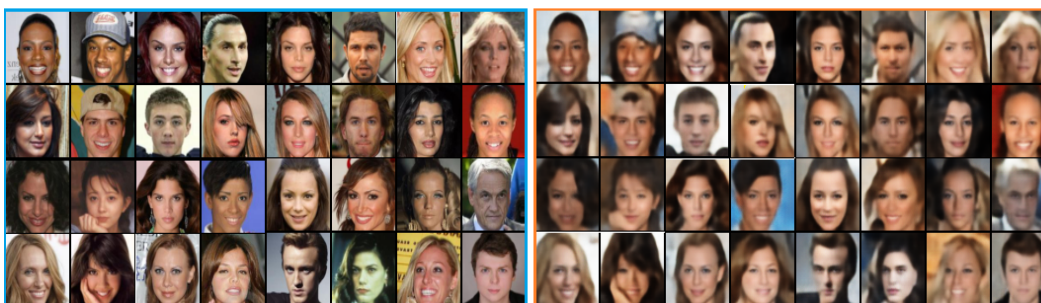


Fig. 4. The comparison of the downstream task models' testing accuracy on centralized (Cen. and with differential privacy C.DP.), federated (with IID Fed., with non-IID F.N., with differential privacy F.N.DP.) and our methods with various size of embedding codes, respectively.



(a) Left is the sample of original images, and right is the reconstructed images to privatize digit ID



(b) Left is the sample of original images, and right is the reconstructed images to privatize identification

Fig. 5. Samples of the original dataset (left) and the corresponding reconstructed version (right) via the DVQ-AE, used to remove information on the digit identity while keeping the circle recognition information, for MNIST and CelebA.

128×3 input size to at most 32×32 latent codes for communication, computing, and storage, achieving comparable accuracy performance as using the raw data. For the speech, the same latent space is 64x smaller than the original waveform input. We also evaluated the normalized amount of time required for training the downstream models for different compression ratios for MNIST, CelebA, and Speech

datasets, and observed a reduction in the required training time across the compression ratios and the models. The reduction can be attributed to the decreasing size of the input data and a smaller number of parameters to learn when applying the OCTOPUS scheme with a suitable compression ratio.

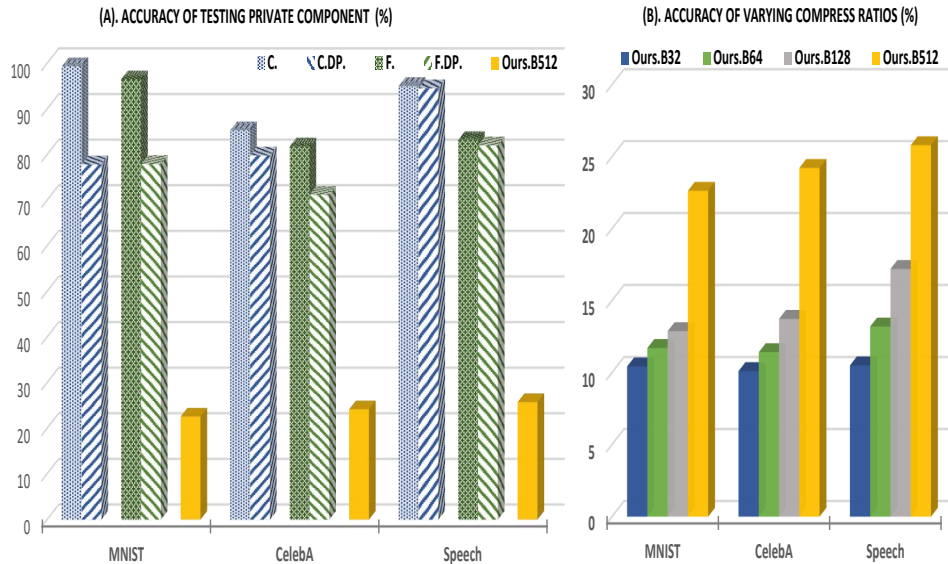


Fig. 6. The comparison of the privacy components' testing accuracy on centralized (Gen. and with differential privacy C.D.P.), federated (with IID Fed., with non-IID F.N., with differential privacy F.N.D.P.) and our methods with various size of embedding codes, respectively.

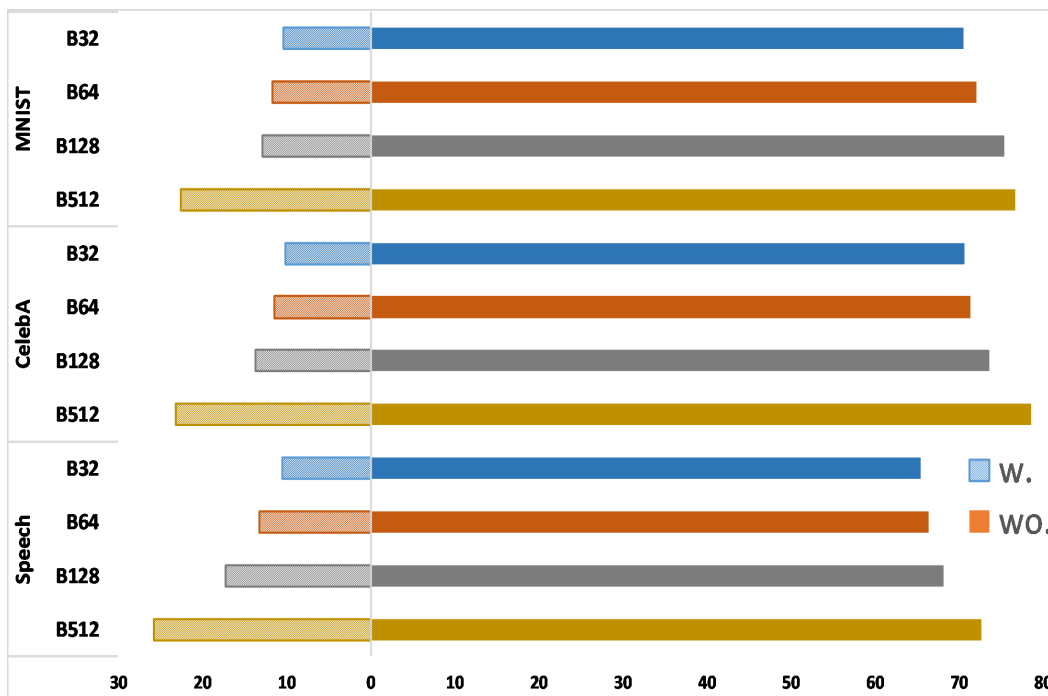


Fig. 7. Accuracy of identifying private component on various size of embedding codes with and without disentanglement strategy.

TABLE 1
Accuracy of identifying private component on various size of embedding codes with and without disentanglement strategy.

w/wo Disent.	B_{32}	B_{64}	B_{128}	B_{512}
MNIST	10.43/70.56	11.71/72.12	12.88/75.45	22.63/76.72
CelebA	10.11/70.65	11.42/71.41	13.73/73.64	23.22/78.62
Speech	10.54/65.42	13.22/66.36	17.21/68.11	25.82/72.64

4 RELATED WORK

Vast amounts of data are necessary to deliver high-quality machine learning models [1]. The conventional framework in Machine Learning considers a centralized dataset connected in the integrated scheme. However, the real-world

data is usually decentralized across multiple parties. Various research works have been conducted in the last few years to apply Federated Learning (FL) to train machine learning models collaboratively while keeping the data decentralized [2], [3], [4].

Generally, a federated learning scheme has fundamentally four principal operations in an iterative manner:

- Sampling Clients. Desired participants are selected by the server from a pool of clients;
- Broadcasting Parameters. The parameters of the initialized commonly-shared model are broadcasted from the server to each selected clients;
- Updating Local Parameters: Each participant retrains

the broadcasting model in a parallel manner using the local data;

- **Aggregating Global Model:** The server will aggregate the gathered uploaded parameters from each client, resulting in the updated global model.

Being a distributed system, Federated Learning also encounters several challenges in terms of communication, system and data heterogeneity, as well as privatization and security. Several FL architectures are developed to address either the accuracy and computational costs or other challenges in the FL field [29], [30], [31], [32], [33].

Even if the models are commonly less expensive to be transmitted than raw data gathering in centralized learning mechanisms, communication burden is one of the main bottlenecks for federated learning. The gradient updates, frequently communicated between nodes in distributed and federated learning, are an inevitable burden, resulting in expensive communication, and scalability constraints [8], [9]. Existing solutions proposed to address the communication overheads are either data compression [34] or by restricting only the relevant outputs by the clients [35], [36] to be uploaded to the parameter server.

The heterogeneity of the data and system in the network, as well as the non-identical nature of the distributed data, impact the performance of the federated learning approaches [25], [29]. Due to lack of global data, there is spatial heterogeneity that each node may have a data value bias and data size variation with respect to the general population, and temporal heterogeneity that the distribution of each local dataset may vary with time. FedAvg is proposed as a solution to address the heterogeneity, however, it is still not robust enough to systems heterogeneity. Enhancements on the model aggregation approaches have also been explored to solve the heterogeneity [37], [38].

Even the raw user data does not leave the local clients, communicating model updates can also reveal sensitive information, requiring additional privacy-preserving strategies, such as secure computation, differential privacy schemes, or running in a trusted execution environment. The common privacy-preserving methods are based on differential privacy to provide a certified privacy guarantee. The differentially private federated learning scheme [14] protects a user’s privacy by adding noise to the clipped model parameters before model aggregation at the cost of model accuracy. Besides, it is time and resource-consuming to conduct perturbation or encryption for the huge amount of parameters with limited resources. And they all fail when the server is untrusted. Additionally, lack of access to global training data can cause security concerns, such as data poisoning or backdoor attacks. As the federated learning scheme being a distributed system, it might be even harder to recognize the misbehaving devices. The attacker can poison the data either by directly inserting poisoned data to the targeted device or injecting poisoned data through other devices [39]. The adversaries could influence either the prediction of a subset of classes or the global model accuracy [40]. To protect the confidentiality of the training data, the aggregator has no visibility into how these updates are generated. A model-poisoning attack is proposed as a more powerful attack than poisoning attacks that target only

the training data [41].

On the other hand, autoencoders (AE) are applied to produce a low-dimensional latent code of the data, aiming to transmit the latent codes to the server instead of raw data. Autoencoders also “encrypt” the data by transforming the raw data into latent vectors, which enhance the security of data. Therefore, autoencoder has been adopted as the feature compression approach to address the communication overhead by only transmitting the encoded vector to the server [10], [11], [12]. However, a separate AE is required to be trained for each local device, which is computationally prohibitive. Additionally, the latent codes still incorporate sensitive information, especially when the server is untrusted.

Consequently, federated learning mechanisms may not be practical in some real-world implementations due to the expensive communication, especially when multiple downstream tasks (e.g., classifiers) should be learned from dynamically updated and non-iid distributed data sources with providing local privatization. To bridge the gap between practice and efficiency, we explore an alternative distributed learning scheme to address the limitations of both federated learning and centralized learning, while enhancing their advantages. To the best of our knowledge, this paper is the first to study to address communication overhead via latent compression, leveraging global data while providing local privatization of local data without additional cost due to encryption or perturbation.

5 CONCLUSION

In this work, we introduce OCTOPUS as a new family of distributed computing frameworks to collect and process distributed data with privatization while enhancing communication, computing aspects, and storage performance in one single task. We demonstrate that OCTOPUS is capable of encoding and transmitting high-dimensional data via compressed latent codes, privatizing local data without extra encryption and perturbation, taking advantage of global data with smaller storage and computing resources. All these experiments demonstrated that the OCTOPUS achieves likelihoods that are almost as good as centralized learning but with privatization and efficient communication on both image and speech data. We demonstrate that OCTOPUS is the efficient distributed learning scheme that can successfully address the communication, computing and storage performance, and privatization of local data in one single task. Such an architecture and procedure enables small devices such as mobile phones or home assistants (e.g. Google home mini) to run a light weight learning algorithm to privatize data under various settings on the fly.

For future work, the exploration on other types of autoencoder to extract latent variables and use of knowledge distillation to help mitigate the reduction in the model accuracy will be explored. Besides, we focus on the single-domain data at the current step, and then move to the multi-domain data (ImageNet) in the future, where the bottleneck is data scale and computation sources instead of method.

REFERENCES

- [1] S. Vaswani, F. Bach, and M. Schmidt, "Fast and faster convergence of sgd for over-parameterized models and an accelerated perceptron," in *The 22nd International Conference on Artificial Intelligence and Statistics*. PMLR, 2019, pp. 1195–1204.
- [2] T. Vogels, S. P. Karimireddy, and M. Jaggi, "Powersgd: Practical low-rank gradient compression for distributed optimization," in *Advances in Neural Information Processing Systems*, 2019, pp. 14 259–14 268.
- [3] J. Konečný, H. B. McMahan, D. Ramage, and P. Richtárik, "Federated optimization: Distributed machine learning for on-device intelligence," *arXiv preprint arXiv:1610.02527*, 2016.
- [4] J. Konečný, H. B. McMahan, F. X. Yu, P. Richtárik, A. T. Suresh, and D. Bacon, "Federated learning: Strategies for improving communication efficiency," *arXiv preprint arXiv:1610.05492*, 2016.
- [5] S. U. Stich, "Local sgd converges fast and communicates little," *arXiv preprint arXiv:1805.09767*, 2018.
- [6] A. Khaled, K. Mishchenko, and P. Richtárik, "Tighter theory for local sgd on identical and heterogeneous data," in *International Conference on Artificial Intelligence and Statistics*. PMLR, 2020, pp. 4519–4529.
- [7] D. Basu, D. Data, C. Karakus, and S. N. Diggavi, "Qsparse-local-sgd: Distributed sgd with quantization, sparsification, and local computations," *IEEE Journal on Selected Areas in Information Theory*, vol. 1, no. 1, pp. 217–226, 2020.
- [8] Y. Lin, S. Han, H. Mao, Y. Wang, and W. J. Dally, "Deep gradient compression: Reducing the communication bandwidth for distributed training," *arXiv preprint arXiv:1712.01887*, 2017.
- [9] H. Zhang, J. Li, K. Kara, D. Alistarh, J. Liu, and C. Zhang, "Zipml: Training linear models with end-to-end low precision, and a little bit of deep learning," in *International Conference on Machine Learning*. PMLR, 2017, pp. 4035–4043.
- [10] O. Fagbohunge, S. R. Reza, X. Dong, and L. Qian, "Efficient privacy preserving edge computing framework for image classification," *arXiv preprint arXiv:2005.04563*, 2020.
- [11] M. Li, W. Zuo, S. Gu, D. Zhao, and D. Zhang, "Learning convolutional networks for content-weighted image compression," in *Proceedings of the IEEE Conference on Computer Vision and Pattern Recognition*, 2018, pp. 3214–3223.
- [12] E. Diao, J. Ding, and V. Tarokh, "Drasic: Distributed recurrent autoencoder for scalable image compression," in *2020 Data Compression Conference (DCC)*. IEEE, 2020, pp. 3–12.
- [13] K. Bonawitz, V. Ivanov, B. Kreuter, A. Marcedone, H. B. McMahan, S. Patel, D. Ramage, A. Segal, and K. Seth, "Practical secure aggregation for federated learning on user-held data," *arXiv preprint arXiv:1611.04482*, 2016.
- [14] R. C. Geyer, T. Klein, and M. Nabi, "Differentially private federated learning: A client level perspective," *arXiv preprint arXiv:1712.07557*, 2017.
- [15] Z. Szabó, B. Póczos, and A. Lőrincz, "Online group-structured dictionary learning," in *CVPR 2011*. IEEE, 2011, pp. 2865–2872.
- [16] L. Kaiser, A. Roy, A. Vaswani, N. Parmar, S. Bengio, J. Uszkoreit, and N. Shazeer, "Fast decoding in sequence models using discrete latent variables," *arXiv preprint arXiv:1803.03382*, 2018.
- [17] R. Rakhimov, D. Volkhonskiy, A. Artemov, D. Zorin, and E. Burnaev, "Latent video transformer," *arXiv preprint arXiv:2006.10704*, 2020.
- [18] J. Chorowski, R. J. Weiss, S. Bengio, and A. van den Oord, "Unsupervised speech representation learning using wavenet autoencoders," *IEEE/ACM transactions on audio, speech, and language processing*, vol. 27, no. 12, pp. 2041–2053, 2019.
- [19] D.-Y. Wu and H.-y. Lee, "One-shot voice conversion by vector quantization," in *ICASSP 2020-2020 IEEE International Conference on Acoustics, Speech and Signal Processing (ICASSP)*. IEEE, 2020, pp. 7734–7738.
- [20] A. Van Den Oord, O. Vinyals *et al.*, "Neural discrete representation learning," in *Advances in Neural Information Processing Systems*, 2017, pp. 6306–6315.
- [21] A. Razavi, A. van den Oord, and O. Vinyals, "Generating diverse high-fidelity images with vq-vae-2," in *Advances in Neural Information Processing Systems*, 2019, pp. 14 866–14 876.
- [22] Y. LeCun and C. Cortes, "MNIST handwritten digit database," 2010. [Online]. Available: <http://yann.lecun.com/exdb/mnist/>
- [23] Z. Liu, P. Luo, X. Wang, and X. Tang, "Deep learning face attributes in the wild," in *Proceedings of International Conference on Computer Vision (ICCV)*, December 2015.
- [24] A. v. d. Oord, S. Dieleman, H. Zen, K. Simonyan, O. Vinyals, A. Graves, N. Kalchbrenner, A. Senior, and K. Kavukcuoglu, "Wavenet: A generative model for raw audio," *arXiv preprint arXiv:1609.03499*, 2016.
- [25] B. McMahan, E. Moore, D. Ramage, S. Hampson, and B. A. y Arcas, "Communication-efficient learning of deep networks from decentralized data," in *Artificial Intelligence and Statistics*. PMLR, 2017, pp. 1273–1282.
- [26] Y. Zhao, M. Li, L. Lai, N. Suda, D. Civin, and V. Chandra, "Federated learning with non-iid data," *arXiv preprint arXiv:1806.00582*, 2018.
- [27] Y. Lu, A. Kumar, S. Zhai, Y. Cheng, T. Javidi, and R. Feris, "Fully-adaptive feature sharing in multi-task networks with applications in person attribute classification," in *Proceedings of the IEEE conference on computer vision and pattern recognition*, 2017, pp. 5334–5343.
- [28] R. Torfason, E. Agustsson, R. Rothe, and R. Timofte, "From face images and attributes to attributes," in *Asian Conference on Computer Vision*. Springer, 2016, pp. 313–329.
- [29] T. Li, A. K. Sahu, A. Talwalkar, and V. Smith, "Federated learning: Challenges, methods, and future directions," *IEEE Signal Processing Magazine*, vol. 37, no. 3, pp. 50–60, 2020.
- [30] M. Aledhari, R. Razzak, R. M. Parizi, and F. Saeed, "Federated learning: A survey on enabling technologies, protocols, and applications," *IEEE Access*, vol. 8, pp. 140 699–140 725, 2020.
- [31] V. Mothukuri, R. M. Parizi, S. Pouriyeh, Y. Huang, A. Dehghan-tanha, and G. Srivastava, "A survey on security and privacy of federated learning," *Future Generation Computer Systems*, vol. 115, pp. 619–640, 2021.
- [32] Q. Yang, Y. Liu, T. Chen, and Y. Tong, "Federated machine learning: Concept and applications," *ACM Transactions on Intelligent Systems and Technology (TIST)*, vol. 10, no. 2, pp. 1–19, 2019.
- [33] P. M. Mammen, "Federated learning: Opportunities and challenges," *arXiv preprint arXiv:2101.05428*, 2021.
- [34] J. Konečný, H. B. McMahan, F. X. Yu, P. Richtárik, A. T. Suresh, and D. Bacon, "Federated learning: Strategies for improving communication efficiency," *arXiv preprint arXiv:1610.05492*, 2016.
- [35] K. Hsieh, A. Harlap, N. Vijaykumar, D. Konomis, G. R. Ganger, P. B. Gibbons, and O. Mutlu, "Gaia: Geo-distributed machine learning approaching {LAN} speeds," in *14th {USENIX} Symposium on Networked Systems Design and Implementation ({NSDI} 17)*, 2017, pp. 629–647.
- [36] W. Luping, W. Wei, and L. Bo, "Cmfl: Mitigating communication overhead for federated learning," in *2019 IEEE 39th International Conference on Distributed Computing Systems (ICDCS)*. IEEE, 2019, pp. 954–964.
- [37] K. Bonawitz, H. Eichner, W. Grieskamp, D. Huba, A. Ingerman, V. Ivanov, C. Kiddon, J. Konečný, S. Mazzocchi, H. B. McMahan *et al.*, "Towards federated learning at scale: System design," *arXiv preprint arXiv:1902.01046*, 2019.
- [38] Y. Liu, J. James, J. Kang, D. Niyato, and S. Zhang, "Privacy-preserving traffic flow prediction: A federated learning approach," *IEEE Internet of Things Journal*, vol. 7, no. 8, pp. 7751–7763, 2020.
- [39] G. Sun, Y. Cong, J. Dong, Q. Wang, and J. Liu, "Data poisoning attacks on federated machine learning," *arXiv preprint arXiv:2004.10020*, 2020.
- [40] V. Tolpegin, S. Truex, M. E. Gursoy, and L. Liu, "Data poisoning attacks against federated learning systems," in *European Symposium on Research in Computer Security*. Springer, 2020, pp. 480–501.
- [41] E. Bagdasaryan, A. Veit, Y. Hua, D. Estrin, and V. Shmatikov, "How to backdoor federated learning," in *International Conference on Artificial Intelligence and Statistics*. PMLR, 2020, pp. 2938–2948.



Shuo Wang Dr. Shuo Wang is a Research Fellow in the CSIRO's Data61 and Cybersecurity CRC. Before joining CSIRO, his Ph.D. and earlier research work was in the School of Computing and Information Systems, University of Melbourne. His main research interests include the areas of: Adversarial Machine Learning: attacks and defenses of deep neural networks; Computer security and privacy, including security and privacy issues in systems, networking, and databases.



Surya Nepal Dr. Surya Nepal is a Principal Research Scientist working on trust and security aspects of Web Services at CSIRO's Data61. His main research interest is in the development and implementation of technologies in the area of Web Services and Service-Oriented Architectures. At CSIRO, Surya researched multimedia databases, Web Services and Service-Oriented Architectures, security, privacy and trust in a collaborative environment.



Kristen Moore Dr. Kristen Moore is a Senior Research Scientist at Data61 and the Cyber Security CRC, working on cyber deception. Previously she was employed as a data scientist at Telstra and Gro Intelligence, where she worked on a broad range of domains and use cases. She completed her PhD in geometric analysis at the Max Planck Institute for Gravitational Physics. Her broad research interests are in Artificial Intelligence (AI) and Machine Learning (ML).



Marthie Grobler Dr. Marthie Grobler currently holds a position as Senior Research Scientist at CSIRO's Data61 in Melbourne, Australia where she leads the human-centric cybersecurity team, driving the work on cybersecurity governance, policies, and awareness.



Carsten Rudolph Carsten Rudolph is an Associate Professor of the Faculty of IT at Monash University, Melbourne, Australia, and Director of the Oceania Cyber Security Centre OCSC. Carsten Rudolph has contributed extensively to four key areas of cybersecurity: Trusted Computing, Security of critical infrastructures and Security of IT Networks; Security by design/security engineering / formal methods for security; Validation and design of security protocols; Digital forensic readiness and secure digital evidence.



Alsharif Abuadbba Dr. Alsharif Abuadbba currently holds a position as Research Scientist at CSIRO's Data61, Australia. He has a PhD in computer security from RMIT university, Melbourne, Australia 2017. He was the winner of RMIT prestigious VC award of Research Excellence in Technology 2018. He was also the winner of Eureka innovation award 2018 for his cybersecurity startup named EyeCura. Dr Alsharif has joined Data61 Distributed System Security group early 2019 as a Research Scientist and Cybersecurity CRC fellow.